

---

## Fitness of teratological morphotypes and heritability of deformities in the diatom *Gomphonema gracile*

Coquillé Nathalie <sup>1, 2, 3, 4</sup>, Morin Soizic <sup>1, \*</sup>

<sup>1</sup> Irstea, UR EABX, 50 avenue de Verdun, 33612 Cestas Cedex, France

<sup>2</sup> Ifremer, Laboratoire d'écotoxicologie, rue de l'île d'Yeu, BP 21105, 44311 Nantes Cedex 03, France

<sup>3</sup> Université de Bordeaux, UMR EPOC 5805 CNRS, LPTC, 351 Cours de la Libération, CS 10004, 33405 Talence Cedex, France

<sup>4</sup> CNRS, UMR 5805, EPOC, LPTC, 351 Cours de la Libération, CS 10004, 33405 Talence Cedex, France

\* Corresponding author : Soizic Morin, email address : [soizic.morin@irstea.fr](mailto:soizic.morin@irstea.fr)

---

### Abstract :

Diatom teratologies have intrigued scientists since the XIXth century, with respect to their causes and origins. These deformities, mainly observed in long-term cultures or under high levels of pollution, were poorly considered, until they were recently found to be potential indicators of toxic impairment of freshwaters. However, very little is known about their ecology.

In this study, the growth and fitness of morphologically distinct descendants of the same cell line of *Gomphonema gracile* (teratological vs. non teratological forms) were compared over a typical growth cycle. Contrary to expectations, teratological populations grew slightly faster, at a rate of  $0.47 \pm 0.03$  divisions.day<sup>-1</sup>, versus  $0.41 \pm 0.04$  for the normal morphotype. They had similar physiological performances as non-teratological forms. They did not differ in their movement velocities, but the trajectory of teratological forms was more linear, likely as a consequence of their elongated outline. Under the same culture conditions, no competitive exclusion of one phenotype over the other was demonstrated on the time scale of an exponential growth cycle (9 days). Moreover, the deformities were faithfully reproduced over time, and no evidence of decreased viability in teratological forms was provided.

These new insights call into question the common hypothesis that deformed diatoms are altered individuals produced by unfavorable conditions and thus highlight ecosystem dysfunction. They call for further investigations of their ecology.

### Highlights

- The growth, physiology and behavior of normal and deformed *Gomphonema gracile* were analyzed.
- Teratological diatoms were able to survive and reproduce. ► Teratology was faithfully passed on with cell division over 9 days. ► Deformed individuals performed similarly to normal ones.

---

**Keywords** : *Gomphonema gracile*, Morphology-based assessment, Teratology, Transmissibility of morphological characters, Phenotypic variability, Fitness

## 1. Introduction

Diatoms are unicellular brown microalgae with an important ecological role in the functioning of freshwaters (Morin et al., 2016). Diatom species identification is based on the morphological features of their siliceous cell wall, the frustule: valve shape and symmetry, cell dimensions, length:width ratio, specific ornamentations (presence and number of raphes, orientation and density of striae, etc.). Practically, diatom identification assumes that the features of the frustule are constant for a given species. A range of length and width variability exists, as the result of the natural morphological variation in diatoms occurring over their life cycle, consequence of their peculiar reproduction cycle (Mann, 2011).

Besides morphological variations associated with development, polymorphism can also result from environmental stress (phenotypic variation) or natural genetic variability (Håkansson and Chepurinov, 1999). Notably, Rose & Cox (2014) documented morphological changes over the life cycle in clones of *Gomphonema parvulum*, complicating the definition of clear species boundaries. Continued culturing resulted in cell size reduction and changes in morphology, potentially leading to the identification of 3 different species. Polymorphism can be an adaptive response of diatom species to a shift in environmental conditions and can result from changing selective pressures (Kociolek and Stoermer, 2010). Trobajo (2007) also detected changes in the morphology of *Nitzschia frustulum* stemming from environmental variations; diatoms were significantly more elongate under increasing salinities and nitrogen concentrations. Frustule deformities or teratologies (abnormal outline or ornamentations) are beyond normal phenotypic variations. They can be induced during valve formation, either by inimical conditions or under long-term artificial culture conditions (see review in Falasco et al., 2009a). Numerous observations of deformed diatoms in laboratory cultures were attributed to cell crowding (Barber and Carter, 1981) or culture senescence (Falasco et al., 2009a). Recently, Windler et al. (2014) reported the major influence of bacteria associated with diatoms in the long-term maintenance of laboratory cultures. They found that cultivation under axenic conditions reduced population growth and promoted morphological changes (cell size reduction, frustule aberrations) in pennate diatoms, compared to xenic cultures.

The teratological character is, thus, commonly accepted to result from unhealthy conditions, as discussed in Lavoie et al. (2017), either in laboratory cultures (lack of essential accompanying bacteria, Windler et al., 2014) or in the field (induction by toxic contamination, Falasco et al., 2009a). For this reason, lower fitness is expected in teratological diatoms, and some types of deformities are even suspected to be lethal (Arini et al., 2013). The assumption that abnormal diatoms may be outcompeted by normal phenotypes under optimal conditions, and ultimately eliminated from the populations, is based on the following empirical observations. First, their rare occurrences: teratologies are infrequent and generally recorded at relative abundances not exceeding 1% (Morin et al., 2012a), in particular under field conditions. Second, they generally appear under altered environments, and were shown to progressively disappear with a return to normal conditions. For instance, Arini et al. (2013) observed that the abundances of cadmium-induced teratologies in *Planothidium frequentissimum* decreased with decontamination. Consistently, the recovery of normal morphology after sexual reproduction in deformed diatoms from long-term cultures suggests that teratologies do not result from genetic drift (Granetti, 1968). Still, the fact that teratological forms are rarely dominant in samples has until now limited the possibility to experimentally validate the hypothesis of competitive exclusion of deformed phenotypes over time.

Given this background, an experiment was carried out to assess the heritability of the teratological character and the viability of abnormal cells. To this end, cell lines descending from laboratory-cultured *Gomphonema gracile* which had diverged into two morphological

variants were used: a normal phenotype and a markedly deformed one. The objectives of this study were: 1) to compare the fitness of both phenotypes under the same culture conditions, and 2) to assess the heritability of the teratological character in diatoms, taking into account the potential influence of closely-associated bacteria. To reach these objectives, both cultures were assessed over 9 days for population dynamics (viability, growth kinetics), cell morphology (cell dimensions, altered frustule), physiology (photosynthesis) and behavior (mobility features). The first hypothesis was that the deformities would be reproduced with cell duplications, while normal phenotypes would be restored with sexual reproduction. The second hypothesis was that the teratological character, even if heritable, would alter the global metabolism of the species, which would be observable through reduced performances in the endpoints studied.

## 2. Materials & Methods

### 2.1. Biological material.

A pennate diatom was isolated from a field sample (Rebec, upstream section of the Leyre river, Southwest France) in December 2013 and established in culture (Coquillé et al., 2015). During the first month that they were cultured (March 2014), cells exhibited typical features of *Gomphonema gracile* Ehrenberg (Reichardt, 2015). Approximately one year later, the parental line of *G. gracile* (further named GGRA) gave rise to two morphologically distinct (but homogenous within one culture) descendant cell lines continuing to reproduce vegetatively. The first phenotype, called GNF (*Gomphonema* normal form), was smaller than the parent culture, less lanceolate and had more rounded apices. The second one, called GTF (*Gomphonema* teratological form), was 2-fold larger than GNF, and all cells exhibited a typical deformity in valve outline ("boomerang shaped", Type 1 deformity in Falasco et al., 2009b).

Before the experiment, GNF and GTF populations were almost pure. They were maintained in separate cultures in sterile Dauta medium (Dauta, 1982) at 17°C in a thermostatic chamber 610 XAP (LMS LTD®, UK) at  $67 \pm 0 \mu\text{mol}\cdot\text{m}^{-2}\cdot\text{s}^{-1}$  with a dark:light cycle of 8:16 h. Non-axenic cultures were grown in 100-mL round borosilicate sterile glass flasks previously heated to 450°C for 6 h and autoclaved 20 min at 121°C.

### 2.2. Experimental design.

The experiment, carried out in March 2015, was run during nine days under the conditions affording *Gomphonema*'s growth without nutrient depletion over time, as used in Coquillé et al. (2015). GNF and GTF cultures were inoculated at 30,000 cells.mL<sup>-1</sup> in sterile Dauta medium (40 mL final volume). As it was likely that a small percentage of the other phenotype would be found in those cultures, the experimental cultures were labelled Ctrl (control) and Trtg (teratological), respectively, in order to avoid confusion between phenotypes and treatments. Triplicate cultures were used for each treatment (Ctrl and Trtg) and incubated simultaneously in a thermostatic chamber 610 XAP (LMS LTD®, UK), under the same environmental conditions as the mother cultures.

On days 1, 2, 3, 6, 7, 8 and 9, population dynamics (viability, growth kinetics), cell morphology (cell dimensions, deformities), physiology (photosynthesis) and behavior (mobility features) were analyzed. On each sampling day, parameters derived from chlorophyll-a fluorescence were first measured, directly on the cultures. Then, the flasks were gently shaken to homogenize the suspensions before sampling 1 mL of culture under the flame. The sample was then aliquoted as follows: 125  $\mu\text{L}$  for the quantitative analysis of live and dead diatoms, 100  $\mu\text{L}$  for mobility measurements, and 200  $\mu\text{L}$  to prepare permanent diatom slides. On the last day of the experiment (day 9), 3 mL of homogenized suspension was used to perform

Rapid Light Curves and the remaining volume of culture was softly filtered on previously ashed Whatman GF/C® filters that were immediately frozen at -20°C before molecular analyses of the associated bacteria.

### 2.3. Chlorophyll-a fluorescence-related endpoints.

Parameters derived from chlorophyll-a fluorescence were measured on the intact biofilms, by means of a PHYTO-PAM (Heinz Walz, GmbH, Germany) equipped with an emitter-detector unit (PHYTO-EDF). Benthic settlement potentially leads to the formation of cell aggregates; therefore ten randomly selected measurements of the effective quantum yield (photosynthetic efficiency) and chlorophyll-a content estimated by chlorophyll-a fluorescence were performed. To do this, a home-made system was used for reproducible direct measurements on the bottom of the flasks. The median of 10 values per sample was then used for statistical analyses.

On day 9, 3 mL of suspension were used to perform Rapid Light Curves (RLC, White and Critchley, 1999) generated with the PHYTO-PAM in ED mode. Briefly, samples adapted to low light irradiance ( $50 \mu\text{mol}\cdot\text{m}^{-2}\cdot\text{s}^{-1}$ ) for 20 minutes were sequentially exposed to increasing actinic irradiances (9 light levels ranging from 64 to  $1,964 \mu\text{mol}\cdot\text{m}^{-2}\cdot\text{s}^{-1}$ ) for 10 seconds, separated by a saturating flash. The relative electron transport rate of photosystem II in response to the light pulse was then plotted against irradiance. The following parameters were extracted from the curves fitted on the model of Eilers & Peeters (1988): photosynthetic efficiency at low light intensity (initial slope of the curve), maximal electron transport rate and onset of light saturation.

### 2.4. Determination of population growth kinetics.

Diatom counts were carried-out on fresh material in a Nageotte counting chamber, using light microscopy at 400x magnification (Olympus BX51, Olympus Optical Co. GmbH, Germany). Diatom cell density and mortality were estimated for each replicate sample as described in Morin et al. (2010). Solitary cells and those forming associations in the counts were distinguished. Density data were recorded as  $\text{cells}\cdot\text{mL}^{-1}$  and the logarithmic increase in population was plotted as a function of time unit, to calculate growth rates (GR, expressed in  $\text{divisions}\cdot\text{day}^{-1}$  during exponential growth) following the formula provided in Morin et al. (2008), and the carrying capacity (i.e. maximum size reached during the stationary phase) of the cultures.

### 2.5. Mobility features.

The percentage of motile cells, as well as their velocity and trajectory, were determined using CASA (computer-assisted sperm analysis) plug-in (Wilson-Leedy and Ingermann, 2007) of ImageJ software under the specific measurement conditions adapted to *G. gracile* by Coquillé et al. (2015). A 20- $\mu\text{L}$  drop of sample was deposited onto a microscope slide and video acquisition (Archimed™, Microvision Instruments) was performed after 2–3 min. Velocity average path (VAP), velocity curvilinear (VCL), velocity straight line (VSL) and linearity ( $\text{LIN} = \text{VSL}/\text{VAP}$ , describing the curvature of the trajectory) (Rurangwa et al., 2004) were then calculated from 260 frames corresponding to 10 seconds of film in total.

### 2.6. Diatom cell morphology.

Organic matter in the samples was removed by adding hydrogen peroxide to the diatom suspensions and kept overnight at room temperature. They were then rinsed with distilled water and centrifuged, before preparing permanent slides according to EN 14407:2014, by mounting the clean samples in Naphrax (provided by Brunel Microscopes Ltd, UK). Then, they

were observed at 1,000x magnification (Leica DMRB, Germany), for the determination of the percentage of normal (symmetrical) and deformed (asymmetrical) *Gomphonema* individuals, based on >100 individuals per replicate sample. Additionally, at least 10 measurements of cell linear dimensions (length, width, thickness) and of striae density were performed in each replicate sample. Average cell biovolume was then calculated using the mathematical equation of Hillebrand et al. (1999) for weakly heteropolar forms (elliptic cylinder).

A return to the origin material (i.e. samples from Coquillé et al., 2015) was made in order to measure, in the same way, the morphological characters of GGRA cells, thus providing elements for comparison and understanding of the morphological range of variation of this culture after 1 year.

### 2.7. Bacterial fingerprinting.

Each replicate filter collected on day 9 was used to analyze the bacterial communities closely associated with the diatoms, i.e. embedded in their extracellular polysaccharides (EPS). Nucleic acids were extracted with the FastDNA SPIN kit for soils (MP Biomedicals, France) and the 16S–23S intergenic spacer region from the bacterial rRNA operon was amplified as described in Pesce et al. (2016), using the universal primers S-D-Bact-1522b-S-20 and L-D-Bact-132-a-A-18. Automated ribosomal intergenic spacer analyses (ARISA) were performed on an Agilent 2100 Bioanalyzer (Agilent Technologies, France) and the resulting profiles were exported from the Agilent 2100 Expert software.

### 2.8. Data analysis.

All statistical analyses were performed with R 3.2.2 (Ihaka and Gentleman, 1996).

After having checked for normality and homogeneity of variances, linear models for fixed effects (lm) were implemented (nlme package). For each endpoint, the effect of culture (Ctrl vs. Trtg), date, and their interaction, were tested sequentially by the model. The results are illustrated as figures in the manuscript. Detailed values and statistics output can be found in Appendix 1.

A t-test was used to compare the parameters extracted from the curves fitted for growth kinetics and RLC between cultures. Additionally, for growth, the kinetics of the two phenotypes in each culture were compared.

For all analyses, a *p*-value below 0.05 was considered statistically significant.

The endpoints raising significant culture and/or date effects were plotted in a Principal Component Analysis (PCA), followed by Hierarchical Clustering to identify the main groups of data, using the FactoMineR package (Lê et al., 2008).

## 3. Results

### 3.1. Diatom morphology: cell dimensions and teratology

During the first months of culture (2014), cells from the original material (GGRA) were identified as small specimens of *Gomphonema gracile*. Valves were quite isopolar in outline and were  $28.91 \pm 0.12 \mu\text{m}$  long and  $5.94 \pm 0.04 \mu\text{m}$  wide (Figure 1). Striking differences were observed between the parental line (GGRA) and the cultures used in this study (Figure 1). Indeed, GNF individuals were slightly more heteropolar with more rounded apices and valves were smaller ( $21.92 \pm 0.09 \mu\text{m}$  long and  $5.92 \pm 0.03 \mu\text{m}$  wide). Moreover, GTF cells were more lanceolate

( $33.88 \pm 0.10 \mu\text{m}$  long and  $6.17 \pm 0.03 \mu\text{m}$  wide) but showed a deformed valve outline (boomerang shape, Figure 2). In all cases, the invagination of the frustule was located opposite to the stigma present in the central area. No difference in the density of striae was found, with average values of  $17.00 \pm 0.09$  striae in  $10 \mu\text{m}$  ( $n=200$ ).

As a consequence of these differences in linear dimensions, the cell biovolumes calculated over the duration of the experiment (7 days for GGRA and 9 days for GTF and GNF) showed significant differences ( $p < 0.001$ ) between GGRA ( $457 \pm 14 \mu\text{m}^3$ ,  $n=150$ ), GNF ( $334 \pm 11 \mu\text{m}^3$ ,  $n=210$ ) and GTF ( $543 \pm 16 \mu\text{m}^3$ ,  $n=210$ ). Cell biovolume of both descendant cell lines tended to slightly decrease with time, and significantly smaller cell sizes were found on days 6 and 9 ( $p < 0.05$ ) (Figure 3A).

Very few deformed individuals were observed in the Ctrl cultures ( $0.34 \pm 0.12\%$ ,  $n=2617$ ) (Figure 4). Cells were in the size range of GNF individuals, but the deformity was similar in location as in GTF (Figure 4). In Trtg cultures, only  $7.7 \pm 0.7\%$  of the cells ( $n=2693$ ) were not deformed, and were morphologically very close to GNF individuals ( $21.07 \pm 0.38 \mu\text{m}$  long,  $6.00 \pm 0.07 \mu\text{m}$  wide;  $n=65$ ).

### 3.2. Growth kinetics

Significant differences in cell densities were observed as a function of time in both cultures, featuring typical growth kinetics with the stationary phase reached from day 6 (Figure 3B). The percentage of dead diatoms decreased continuously on the first dates, simultaneously to the exponential cell increase. Then, mortality increased when the stationary phase was reached (culture x date interaction,  $p < 0.05$ , Figure 3C).

Despite the absence of any statistical difference in overall growth rates between Ctrl ( $\text{GR} = 0.46 \pm 0.01 \text{ divisions.day}^{-1}$ ) and Trtg cultures ( $\text{GR} = 0.49 \pm 0.04 \text{ divisions.day}^{-1}$ ) in the exponential growth phase ( $p = 0.63$ ), t-tests revealed statistical differences in the specific growth rates of GNF and GTF phenotypes in Ctrl and Trtg cultures (Figure 5,  $p < 0.001$  in both cases). Indeed, GNF populations grew faster in the Ctrl units ( $0.46 \pm 0.01 \text{ divisions.day}^{-1}$ ) than in the Trtg ones ( $0.37 \pm 0.08 \text{ divisions.day}^{-1}$ ), where they reached their stationary phase one day later (day 8 instead of day 7). GTF had the same growth characteristics as GNF in the Ctrl ( $\text{GR} = 0.45 \pm 0.06 \text{ divisions.day}^{-1}$ , stationary phase starting on day 7). Conversely, in the Trtg units, they showed higher division rates ( $0.49 \pm 0.04 \text{ divisions.day}^{-1}$  vs.  $0.37 \pm 0.08 \text{ divisions.day}^{-1}$  for GNF) and consequently attained their maximal cell density earlier (on day 6, Figure 3B). Therefore, significant interaction between culture and date was highlighted for cell densities, as a result of the delay in reaching maximal cell numbers in GNF (on day 7, Figure 3B).

The carrying capacity (maximum population size) in cell density was about one third lower for Trtg cultures ( $397,800 \pm 31,700 \text{ cell.mL}^{-1}$ , average values for days 7 to 9) compared to Ctrl cultures ( $616,200 \pm 44,400 \text{ cell.mL}^{-1}$ , average values for days 7 to 9) (Figure 3B). However, the total biovolume occupied (i.e. cell densities x individual biovolume) did not differ between experimental units from day 7, with an average of  $197 \pm 12.10^6 \mu\text{m}^3.\text{mL}^{-1}$  (Figure 3D).

### 3.3. Physiology

No significant difference was observed in chlorophyll-a derived parameters between Ctrl and Trtg ( $p = 0.42$ ). Chlorophyll-a fluorescence followed a bell-shaped curve and peaked on day 6 (Figure 3E). Photosynthetic activity (Figure 3F) increased on the first days of exponential growth, and then slightly decreased over time (from day 6).

The RLC did not highlight any differences between treatments in the use of light by the cultures (Appendix 2). Indeed, similar values were obtained for Ctrl and Trtg photosynthetic efficiency at low light intensity ( $0.23 \pm 0.00$  in average,  $p=0.09$ ), as well as the maximum electron transport rate ( $95.1 \pm 7.6 \mu\text{mol electrons.m}^{-2}.\text{s}^{-1}$ ,  $p=0.83$ ), reached from the saturating irradiance of  $415.9 \pm 30.1 \mu\text{mol.m}^{-2}.\text{s}^{-1}$  ( $p=0.90$ ).

### 3.4. Behavior

In both cultures, cells grew benthically, and were mostly solitary. Up to  $40 \pm 2\%$  cells (Ctrl, day 2) had the potential to form aggregates, principally forming star-shaped associations (Figure 3G). The abundance of cell clumps was always higher in Ctrl cultures ( $p<0.001$ ) and decreased over time whatever the culture from day 2 ( $p<0.01$ ). For this reason, on the first days, the percentage of mobile diatoms was so low that mobility parameters could not be determined appropriately. When the cultures reached their stationary phase, the percentage of cells forming aggregates drastically decreased and the percentage of mobile cells increased significantly (Figure 3H), simultaneously to a decrease of benthic forms (as assessed through the chlorophyll-*a* settled on the bottom of the flasks, Figure 3E). Striking differences in motility were observed between cultures ( $p<0.001$ ): in the Ctrl, the percentage of mobile cells gradually increased from  $<5\%$  (day 6) to  $18.9 \pm 3.4\%$  (day 9). Oppositely,  $36.8 \pm 2.7\%$  cells were mobile in the Trtg cultures from day 6 to 8, then decreased to  $21.5 \pm 3.4\%$  on the last day of the experiment. On the last days, the percentage of associated cells was low ( $5.6 \pm 2.6\%$  in Ctrl and  $1.3 \pm 0.5\%$  in Trtg cultures), and the cells grew mostly in suspended, loose agglomerates, potentially indicating biofilm senescence. No significant difference was found between cultures with respect to movement velocity; however, the trajectory was more linear in Trtg ( $p<0.05$ ) (Appendix 1).

### 3.5. Global patterns in sample variation

The two first dimensions of the PCA explained the same amount of data variability, reaching 68.43% of combined variance (Figure 6A). The optimal clustering reached after applying the PCA discriminated four groups (Figure 6B).

The first component of the PCA expressed a temporal gradient. It discriminated between samples collected on the first days of sampling (exponential growth phase), located on the left half-panel, and cultures corresponding to the stationary phase (last sampling days), located on the right half-panel. Positive values along this dimension were correlated with increasing carrying capacity (total cell biovolume, cell density) as well as other endpoints related to termination of growth: higher mortality, increasing percentages of mobile cells associated with decreasing cell aggregation.

The second PCA component separated treatments, with Ctrl clustered on the lower half-panel and Trtg on the upper half-panel. Sample discrimination was mostly related to the morphological descriptors (cell dimensions, biovolume, percentage of teratologies), and with more linear trajectories in Trtg on the last days of sampling.

### 3.6. ARISA profiles

Amplification of the 16S rDNA genes on the filters did not give rise to banding patterns in one replicate sample of Ctrl (likely due to an experimental error), which was consequently discarded. Fingerprinting of bacterial communities (Appendix 3) highlighted that Ctrl and Trtg cultures shared 3 major peaks (above a threshold of 100 relative fluorescence units in height from the baseline), and that no major differences were found between Ctrl and Trtg. However,



a minor peak (below 50 fluorescence units) was detected around 623bp, but only in the Trtg samples.

## 4. Discussion

### 4.1. Implications of deformities for fitness and survival

#### 4.1.1. Teratologies did not impact performance in GTF populations

Results of this study are in complete disagreement with common assumptions that deformed individuals are impaired. Indeed, the deformed culture of *Gomphonema gracile* (GTF) did not exhibit a longer lag phase compared to the controls and growth rates of the GTF populations were similar or higher than those of GNF (Figure 5). Growth rates of the GTF population were higher than that of GNF in Trtg cultures, and similar in Ctrl cultures, possibly resulting in higher competitive abilities of GTF individuals, compared to GNF ones, under specific conditions. This is in contradiction with the observations made by Windler et al. (2014), where teratological cultures had grown more slowly than normal cultures. However, it is worth noting that, in their study, teratologies were suspected to result from axenicity, which was not the case here.

The carrying capacity (maximum cell density in the stationary phase) was certainly lower in Trtg than in Ctrl (~400,000 cells.mL<sup>-1</sup> vs. ~600,000 cells.mL<sup>-1</sup>). However, these differences were likely caused by space availability more than growth abilities: total biovolume occupied in the stationary phase was similar in Ctrl and Trtg cultures. In the same way, Windler et al. (2014) observed that their normal and teratological cultures of *Achnanthes minutissimum* reached similar chlorophyll concentrations in the stationary phase. Thus, competition for space (and subsequent access to resources such as nutrients and/or light) was probably the main driving factor in kinetics for both cultures in this experiment.

Besides growth kinetics, the physiological and behavioral endpoints assessed did not show lower performances of GTF populations, contrarily to what was expected. Photosynthetic efficiency was similar in Trtg compared to Ctrl cultures and fell into the range of other measurements carried-out on *G. gracile* (Coquillé et al., 2015; Table 1). In this experiment, the mobility features (percentage of mobile cells and velocities) of GNF and GTF individuals were below the values reported by Coquillé et al. (2015). Nevertheless, differences were found between Ctrl and Trtg: more mobile individuals were found within GTF populations and they moved more linearly than GNF cells (Figure 6). This may be a consequence of their more elongated valve outline. No differences were found, however, in movement velocity, in agreement with Bertrand's work on the motility of several diatom species (1990, 1999). Based on analyses of five distinct populations, he also demonstrated that velocity was independent of cell size within a species (Bertrand, 1990).

To sum up, the morphological changes that occurred in *Gomphonema gracile* did not impair its performance, based on the endpoints assessed, when cultured alone. The fact that GNF and GTF displayed similar responses in cultures where they were dominant does not prejudice their behavior when found together. Superseding of GTF by GNF would be expected based on Arini et al. (2013)'s work, arguing for a relative decrease in the percentage of deformed diatoms under optimal growth conditions.

#### 4.1.2. Coexistence of GNF and GTF morphotypes

The teratological forms had higher growth rates and higher cell dimensions, thus higher cell surface in contact with their environment for nutrient uptake. Moreover, the cells tended to form large floating bulks of solitary individuals, whereas they formed benthic mats in Coquillé et al. (2015). This may stem from ageing with long-term culturing, as well as from the morphological

changes over time in *G. gracile*. These associations were more striking in the GTF cultures; deformed diatoms may thus be less adhesive than the normal forms. This slightly distinct lifestyle can be an adaptation of this phenotype, larger than GNF and more silicified, to modify its sinking rates and/or maximize its access to resources (nutrients, light). Such adaptive mechanisms have been observed in small lacustrine *Stephanodiscus* species (Kocielek and Stoermer, 2010). Therefore, these adaptations may confer a competitive advantage to GTF individuals over the normal morphotype under certain circumstances. The low percentage of non-teratological forms in GTF, stable over time, tends to confirm this hypothesis.

The percentage of deformed individuals in Ctrl fell into the range of the abundances occurring “naturally” in the field, i.e. below 0.35% (Morin et al., 2012a). The GTF phenotype did not significantly increase over time in Ctrl cultures, indicating that GNF was not outcompeted (in agreement with the GR values of GNF and GTF in Ctrl units, Figure 3). However, the differential growth of GNF and GTF in Trtg units suggests that a massive outbreak of teratological individuals, owing to an extreme event and/or repeated toxic exposure, could lead to competitive exclusion of their normal congeners. Neury-Ormanni et al. (2017) performed a competition experiment with a balanced GNF:GTF inoculum under the same physicochemical conditions as in the present study. In their experiment, no significant differences in growth were found, compared to the individual kinetics of GNF and GTF, and both phenotypes co-occurred at a 1:1 ratio until the stationary phase was reached. Therefore, dedicated competition experiments using several GNF:GTF ratios would constitute a potential way to confirm this theory and determine a threshold above which teratological diatoms would irreversibly dominate over normal ones. However, there is evidence from translocation experiments (Tolcach and Gómez, 2002) and laboratory investigations (Morin et al., 2012b) that diatom immigration may contribute to re-colonization when toxic contamination is removed, and mask a small population of deformed individuals kept alive. Indeed, in the field, continuous immigration of normal morphotypes and competition with several other species likely impedes the sustainable presence of teratological diatoms under uncontaminated conditions.

#### 4.2. Transmission of the teratological character over time

##### 4.2.1. Consistency in the teratological feature

In this study, the culture of deformed *Gomphonema gracile* (GTF) was maintained with classical growth kinetics at abundances exceeding 90%, suggesting that the deformity was non-lethal. In long-term cultures, frustule aberrations were demonstrated to increase as valves decrease in length in several diatom species (e.g. Hostetter and Rutherford, 1976; Torgan et al., 2006). In this study, on the contrary, GTF cells were larger than the other population, although at the same development stage as the non-teratological populations (GNF). All deformed diatoms from Trtg and Ctrl exhibited a typical deformed valve outline with symmetry loss (Figure 1 and Figure 2), although the few deformed diatoms in Ctrl were smaller than the GTF populations (Figure 2).

Valve asymmetry is the most frequent type of deformity in *Gomphonema* species (Falasco et al., 2009b). Similarly incised valves have been described as abnormal *G. parvulum* (Victoria and Gómez, 2010) and *G. gracile* (Morin and Coste, 2006) in natural communities under toxic contamination, where they were associated with normal specimens. Indeed, the consistency of this feature reproduced over time in the Trtg units suggested either that a new species emerged (with another strain of associated bacteria as suggested by ARISA profiles; Appendix 3), or that boomerang-shaped outline deformation preferentially occurs in *Gomphonema*.

#### 4.2.2. Heritability of the teratology throughout the experiment

Heritability of teratologies was empirically demonstrated through the reproduction of deformed *Gomphonema gracile* in the Trtg cultures over the 9-day experiment. Indeed, the percentage of GTF cells was stable through time, although cultures grew in cell numbers. This may have resulted from i) mechanical transmission through generations by vegetative division (Round et al., 1990; Von Dassow et al., 2006) of the deformed clones and/or ii) higher growth rates in GTF cultures, potentially masking the recovery of normal forms (with lower growth rates, as inferred by GNF growth kinetics in Trtg cultures; also see section 4.1.1). Restoration of maximal size in GTF on day 7 (Table 1), coinciding with stabilization of cell numbers (plateau phase) and the decrease of benthic cells suggested that they underwent sexual reproduction at the timescale of the 9-day experiment. Even though a slight decrease in the percentages of deformities was observed in GTF after sexual reproduction ( $89.4 \pm 4.0\%$  on day 8, Figure 4), it seems that the genetic and/or epigenetic cause of teratologies is most likely.

Reversibility of teratologies is generally assumed; for instance Granetti (1968) observed in long-term cultures that deformed *Navicula* species restored their normal morphology after sexual reproduction, leading him to discard the genetic cause of teratologies. However, McLaughlin (1988) stated that, if the variation of morphology is well defined, consistent and reproducible, teratologies should be considered as varieties of the species. In line with this, Jüttner et al. (2013) described a *Gomphonema* with a deflection in the head and foot poles as a new species, based on its frequent occurrence and large geographical distribution, thus assuming genetic distinctness. As generally observed in long-term cultures, continuous culturing resulted in a decrease in cell size over time for both phenotypes. Size differences between GNF and GTF populations were perpetuated and maintained for 6 extra months (Ezzedine and Vedrenne, 2015): in August 2015, GNF cells averaged  $17.35 \pm 0.15 \mu\text{m}$  ( $n=160$ ) in length. In the same way, continuous decrease also occurred in GTF populations that were  $29.59 \pm 0.14 \mu\text{m}$  ( $n=320$ ) long. The deformities were not reversed after the predictable rounds of sexual reproduction over this extra 6-month period. The continuity of the teratological feature, repeated throughout the GTF population in varying sizes of individuals, also argues in favor of a new variety (McLaughlin, 1988). Further investigations would thus be required (i) to characterize both GNF and GTF genomes in depth in order to identify the potential mutations, to discard or not the genetic causes of diatom teratologies and (ii) to characterize the two epigenomes via the study of DNA methylation and epigenetic causes of diatom teratologies.

#### 4.2.3. Long term persistence of the teratological feature suggests genetic and/or epigenetic control

In this study, both Ctrl and Trtg cultures were issued from a unique parental line which had diverged morphologically. Initially (i.e. when GTF appeared), deformation of this cell line may have been induced by mechanical causes such as crowding in the cultures or by changes in the accompanying bacteria (rather than axenicity, as bacteria were found in both cultures at the end of the experiment). The ARISA profiles differed slightly between cultures by the presence of one small peak in Trtg, suggesting that another strain of bacteria was present in these cultures. Hypotheses regarding a previous exposure to chemical insults or inappropriate culture conditions can be discarded. Indeed, the diatom was isolated from a pristine site in Rebec tributary, and then cultivated using a culture medium under laboratory conditions that were previously shown to be adapted to *G. gracile*'s growth (Coquillé et al., 2015). Besides, both GNF and GTF morphotypes were cultivated under identical conditions that proved to be appropriate given their growth kinetics, thus endorsing the deformity as teratological.

Although the body of work dealing with diatom teratologies is vast (Falasco et al., 2009a), Lavoie et al. 2017), the processes involved in the formation of abnormal cells are still unclear and it has never been proved whether they resulted or not from epigenetic mechanisms or genetic alteration. Better knowledge at the molecular level and more specifically at the epigenetic level is necessary because of the conservation of the epigenetic machinery in diatoms, its potentially role in phenotypic modification (Tirichine et al., 2017) and, contrary to genetic factors, ease in evaluating some parameters such as DNA methylation. Indeed, the identification of genetic alteration is hardly assessable directly since few genomes have been sequenced and annotated, making it difficult to target the genetic loci responsible for frustule morphology and to identify potential alterations.

## **5. Conclusions**

The phenotypic plasticity in diatoms makes heritability difficult to assess, but thanks to unexpected changes in cultures from the same parental line, cultures of morphological variants of *Gomphonema gracile* (normal and abnormal phenotypes) made it possible to comparatively study them. The results of this study showed that teratologies were reproduced over time in both Ctrl and Trtg cultures, to variable extent depending on the experimental units considered. Moreover, teratology did not significantly affect physiology nor behavior, disputing the previous assumptions that abnormal diatoms are not competitive and are only found as a transient state, useful to point out extremely adverse environmental conditions. Thus, the similarity in the performance of GTF individuals, compared to normal forms (GNF), has implications for the improvement of knowledge about the ecology of teratological diatoms, and for the environmental interpretations made in hydrosystems where they are found. Indeed, this study provides evidence that abnormal diatoms, likely to appear by chance, are viable individuals and may hold out against normal forms under “favorable” conditions. Consequently, much care must be paid to them in biomonitoring studies, before stating that the presence of teratologies reflects the degradation of water quality.

Apart from the ability to transmit teratological characters as seen in the microscopical observations of diatom morphology and discussed in this paper, the growth and physiology data strongly advocate for a genetic and/or epigenetic origin in GTF. In future, special attention should be given to diatom teratologies from the genetic and epigenetic standpoint to understand if they result from alterations in genome and/or epigenetic modifications, to their ecological preferences.

## **6. Acknowledgements**

Authors thank Gwilherm Jan (Irstea Bordeaux) for his precious technical help, Evane Thorel (Irstea Bordeaux) for performing the RLCs, Michel Coste (Irstea Bordeaux) and PLACAMAT (UMS3626) for providing the SEM microphotographs, as well as Christophe Rosy and Bernadette Volat (Irstea Lyon) who performed DNA extraction and bacterial diversity analyses. Emilie Saulnier-Talbot edited this manuscript and provided helpful suggestions. This study was carried out with financial support from the French National Research Agency (ANR) in the framework of the Investments for the Future Programme, within the Cluster of Excellence COTE (ANR-10-LABX-45).

## 7. References

- Arini, A., Durant, F., Coste, M., Delmas, F., Feurtet-Mazel, A., 2013. Cadmium decontamination and reversal potential of teratological forms of the diatom *Planothidium frequentissimum* (Bacillariophyceae) after experimental contamination. *J. Phycol.* 49, 361-370.
- Barber, H.G., Carter, J.R., 1981. Observations on some deformities found in British diatoms. *Microscopy* 34, 214-226.
- Bertrand, J., 1990. La vitesse de déplacement des diatomées. *Diat. Res.* 5, 223-239.
- Bertrand, J., 1999. Mouvements des diatomées VI. Les efforts pendant le déplacement apical. Mesures, analyses, relations : longueur, vitesse, force. *Cryptog. Algol.* 20, 43-57.
- Cantonati, M., Angeli, N., Virtanen, L., Wojtal, A.Z., Gabrieli, J., Falasco, E., Lavoie, I., Morin, S., Marchetto, A., Fortin, C., Smirnova, S., 2014. *Achnantheidium minutissimum* (Bacillariophyta) valve deformities as indicators of metal enrichment in diverse widely-distributed freshwater habitats. *Sci. Total Environ.* 475, 201-215.
- Coquillé, N., Jan, G., Moreira, A., Morin, S., 2015. Use of diatom motility features as endpoints of metolachlor toxicity. *Aquat. Toxicol.* 158, 202-210.
- Coste, M., Boutry, S., Tison-Rosebery, J., Delmas, F., 2009. Improvements of the Biological Diatom Index (BDI): Description and efficiency of the new version (BDI-2006). *Ecol. Indicators* 9, 621-650.
- Dauta, A., 1982. Conditions de développement du phytoplancton. Etude comparative du comportement de huit espèces en culture. I. Détermination des paramètres de croissance en fonction de la lumière et de la température. *Annls Limnol.* 18, 217-262.
- Eilers, P.H.C., Peeters, J.C.H., 1988. A model for the relationship between light intensity and the rate of photosynthesis in phytoplankton. *Ecol. Modelling* 42, 199-215.
- Ezzedine, J., Vedrenne, J., 2015. Le FlowCAM : protocoles appliqués à la différentiation morphologique et au calcul de biovolumes de *Gomphonema gracile*, 34ème Colloque de l'Association des Diatomistes de Langue Française (ADLaF), Bordeaux, p. 24/68.
- Falasco, E., Bona, F., Badino, G., Hoffmann, L., Ector, L., 2009a. Diatom teratological forms and environmental alterations: a review. *Hydrobiologia* 623, 1-35.
- Falasco, E., Bona, F., Ginepro, M., Hlúbiková, D., Hoffmann, L., Ector, L., 2009b. Morphological abnormalities of diatom silica walls in relation to heavy metal contamination and artificial growth conditions. *Water SA* 35, 595-606.
- Gómez, M., Licursi, M., 2003. Abnormal forms in *Pinnularia gibba* (Bacillariophyceae) in a polluted lowland stream from Argentina. *Nova Hedw.* 77, 389-398.
- Granetti, B., 1968. Alcune forme teratologiche comparse in colture di *Navicula minima* Grun. e *Navicula seminulum* Grun. *Giornale botanico italiano* 102, 469-484.
- Håkansson, H., Chepurnov, V., 1999. A study of variation in valve morphology of the diatom *Cyclotella meneghiniana* in monoclonal cultures: effect of auxospore formation and different salinity conditions. *Diat. Res.* 14, 251-272.
- Hillebrand, H., Dürselen, C.D., Kirschtel, D., Pollingher, U., Zohary, T., 1999. Biovolume calculation for pelagic and benthic microalgae. *J. Phycol.* 35, 403-424.
- Hostetter, H.P., Rutherford, K.D., 1976. Polymorphism in the diatom *Pinnularia brebissonii* in culture and a field collection. *J. Phycol.* 12, 140-146.
- Ihaka, R., Gentleman, R., 1996. R: A language for data analysis and graphics. *J. Comput. Graph. Statist.* 5, 299-314.
- Jüttner, I., Ector, L., Reichardt, E., Van de Vijver, B., Jarlman, A., Krokowski, J., Cox, E.J., 2013. *Gomphonema varioeruduncum* sp. nov., a new species from northern and western Europe and a re-examination of *Gomphonema exilissimum*. *Diat. Res.* 28, 303-316.
- Kociolek, J.P., Stoermer, E.F., 2010. Variation and polymorphism in diatoms: the triple helix of development, genetics and environment. A review of the literature. *Vie et Milieu - Life and Environment* 60, 75-87.
- Lavoie, I., Hamilton, P.B., Morin, S., Kim Tiam, S., Gonçalves, S., Falasco, E., Fortin, C., Gontero, B., Heudre, D., Kahlert, M., Kojadinovic-Sirinelli, M., Manoylov, K., Pandey, L., Taylor, J., 2017. Diatom teratologies as biomarkers of contamination: are all deformities ecologically meaningful? *Ecol. Indicators* in press.
- Lê, S., Josse, J., Husson, F., 2008. FactoMineR: An R Package for Multivariate Analysis. *Journal of Statistical Software* 25, 1-18.

- Mann, D.G., 2011. Size and sex, in: Seckbach, J., Kociolek, J.P. (Eds.), The diatom world. Springer Science, pp. 145-166.
- McLaughlin, R.B., 1988. Teratological forms. The Microscope 36, 261-271.
- Morin, S., Corcoll, N., Bonet, B., Tlili, A., Guasch, H., 2014. Diatom responses to zinc contamination along a Mediterranean river. Plant Ecology and Evolution 147, 325-332.
- Morin, S., Cordonier, A., Lavoie, I., Arini, A., Blanco, S., Duong, T.T., Tornés, E., Bonet, B., Corcoll, N., Faggiano, L., Laviale, M., Pérès, F., Becares, E., Coste, M., Feurtet-Mazel, A., Fortin, C., Guasch, H., Sabater, S., 2012a. Consistency in diatom response to metal-contaminated environments, in: Guasch, H., Ginebreda, A., Geiszinger, A. (Eds.), Hdb Env Chem. Springer, Heidelberg, pp. 117-146.
- Morin, S., Coste, M., 2006. Metal-induced shifts in the morphology of diatoms from the Riou Mort and Riou Viou streams (South West France), in: Ács, É., Kiss, K.T., Padisák, J., Szabó, K. (Eds.), Use of algae for monitoring rivers VI. Hungarian Algological Society, Göd, Hungary, Balatonfüred, pp. 91-106.
- Morin, S., Coste, M., Delmas, F., 2008. A comparison of specific growth rates of periphytic diatoms of varying cell size under laboratory and field conditions. Hydrobiologia 614, 285-297.
- Morin, S., Gómez, N., Tornés, E., Licursi, M., Rosebery, J., 2016. Benthic diatom monitoring and assessment of freshwater environments: Standard methods and future challenges, in: Romaní, A.M., Guasch, H., Balaguer, M.D. (Eds.), Aquatic Biofilms: Ecology, Water Quality and Wastewater Treatment. Caister Academic Press, pp. 111-124.
- Morin, S., Lambert, A.-S., Artigas, J., Coquery, M., Pesce, S., 2012b. Diatom immigration drives biofilm recovery after chronic copper exposure. Freshwat. Biol. 57, 1658-1666.
- Morin, S., Proia, L., Ricart, M., Bonnineau, C., Geiszinger, A., Ricciardi, F., Guasch, H., Romaní, A., Sabater, S., 2010. Effects of a bactericide on the structure and survival of benthic diatom communities. Vie Milieu 60, 109-116.
- Neury-Ormanni, J., Vedrenne, J., Morin, S., 2017. Predation, competition, chemical stressors in freshwater biofilm: synergism or antagonism?, SEFS10, Olomouc, CZ.
- Pesce, S., Zoghlami, O., Margoum, C., Artigas, J., Chaumot, A., Foulquier, A., 2016. Combined effects of drought and the fungicide tebuconazole on aquatic leaf litter decomposition. Aquat. Toxicol. 173, 120-131.
- Reichardt, E., 2015. *Gomphonema gracile* Ehrenberg sensu stricto et sensu auct. (Bacillariophyceae): A taxonomic revision. Nova Hedw. 101, 367-393.
- Rose, D.T., Cox, E.J., 2014. What constitutes *Gomphonema parvulum*? Long-term culture studies show that some varieties of *G. parvulum* belong with other *Gomphonema* species. Plant Ecology and Evolution 147, 366-373.
- Round, F.E., Crawford, R.M., Mann, D.G., 1990. The Diatoms. Biology & morphology of the genera. Cambridge Univ.Press Ed.
- Rurangwa, E., Kime, D.E., Ollevier, F., Nash, J.P., 2004. The measurement of sperm motility and factors affecting sperm quality in cultured fish. Aquaculture 234, 1-28.
- Tirichine, L., Rastogi, A., Bowler, C., 2017. Recent progress in diatom genomics and epigenomics. Current Opinion in Plant Biology 36, 46-55.
- Tolcach, E.R., Gómez, N., 2002. The effect of translocation of microbenthic communities in a polluted lowland stream. Verh. Internat. Verein. Limnol. 28, 254-258.
- Torgan, L.C., Vieira, A.A.H., Girollo, D., dos Santos, C.B., 2006. Morphological irregularity and small cell size in *Thalassiosira duostra* maintained in culture, in: Witkowski, A. (Ed.), Proceedings of the 18th International Diatom Symposium. Biopress Ltd., Bristol, UK, pp. 407-416.
- Trobajo Pujadas, R., 2007. Ecological analysis of periphytic diatoms in Mediterranean coastal wetlands (Empordà wetlands, NE Spain). Koeltz Scientific Books, Koenigstein / Germany.
- Victoria, S.M., Gómez, N., 2010. Assessing the disturbance caused by an industrial discharge using field transfer of epipellic biofilm. Sci. Total Environ. 408, 2696-2705.
- Von Dassow, P., Chepurinov, V.A., Armbrust, E.V., 2006. Relationships between growth rate, cell size, and induction of spermatogenesis in the centric diatom *Thalassiosira weissflogii* (Bacillariophyta) J. Phycol. 42, 887-899.
- White, A.J., Critchley, C., 1999. Rapid light curves: A new fluorescence method to assess the state of the photosynthetic apparatus. Photosynth Res 59, 63-72.

Wilson-Leedy, J., Ingermann, R., 2007. Development of a novel CASA system based on open source software for characterization of zebrafish sperm motility parameters. *Theriogenology* 67, 661-672.

Windler, M., Bova, D., Kryvenda, A., Straile, D., Gruber, A., Kroth, P.G., 2014. Influence of bacteria on cell size development and morphology of cultivated diatoms. *Phycological Res.* 62, 269-281.

*Figure captions:*

Figure 1. Diatom cell dimensions (length and width, in  $\mu\text{m}$ ) in the Ctrl (white diamonds,  $n=210$ ) and Trtg (black diamonds,  $n=210$ ) cultures, compared to the parental culture (GGRA, grey diamonds,  $n=150$ ). Significant differences in length were found between Ctrl and Trtg ( $p<0.001$ ).

Figure 2. External (left) and internal (right) views of teratological valves from GTF cultures (SEM microphotographs).

Figure 3. Temporal evolution in Ctrl (white diamonds) and Trtg (black diamonds) cultures of A- Individual cell biovolumes ( $\mu\text{m}^3$ ), B- Diatom cell densities ( $\text{cells.mL}^{-1}$ ), C- Mortality (%), D- Total cell biovolume ( $\mu\text{m}^3$  per mL), E- Photosynthetic efficiency (relative units r.u.), F- Chlorophyll-a measured on the bottom of the flasks ( $\mu\text{g.cm}^{-2}$ ), G- Percentage of cells forming associations (%) and H- Percentage of mobile cells (%). n.d. = not determined because the number of mobile individuals was too low). Linear mixed-effects models highlight a significant culture effect (\*) for individual biovolumes (A,  $p<0.001$ ), significant date effects (†) for individual biovolumes (A,  $p<0.05$ ), photosynthetic efficiency (E,  $p<0.05$ ) and chlorophyll-a content (F,  $p<0.001$ ), while interactive effects between culture and date (‡) are found for growth kinetics (cell densities B,  $p<0.001$ ; total cell biovolume C,  $p<0.001$  and mortality D,  $p<0.05$ ) and the percentage of cells in associations or motile (G and H,  $p<0.01$ ).

Figure 4. Teratological forms. Left panel: Percentage of deformed individuals (%) in Ctrl (white diamonds,  $n=2617$ ) and Trtg (black diamonds,  $n=2693$ ) cultures. \* denotes a significant culture effect ( $p<0.001$ ) identified by the linear mixed-effects model. Right panel: Light microscopy photomicrographs of the teratological *Gomphonema* found in Ctrl (down) and in Trtg cultures (top). Scale bar:  $10\ \mu\text{m}$ .

Figure 5. Population dynamics of GNF and GTF phenotypes during the experiment, in the Ctrl (A) and Trtg (B) cultures. Experimental results are shown by: open symbols, GNF; solid symbols, GTF. The dashed and solid lines indicate the best-fitting growth curves for normal (GNF) and teratological (GTF) forms, respectively; growth rates (GR, in  $\text{divisions.day}^{-1}$ ) and duration of exponential phase considered are specified for each data series. Note the logarithmic scale on the Y-Axis.

Figure 6. Principal component analysis (PCA) based on the endpoints significantly affected by treatment (culture) and/or date. A- Variables factor map. B- Projection of the individuals, labelled according to a *posteriori* clustering outputs. Grey arrows show temporal changes for both cultures.



Fig. 1

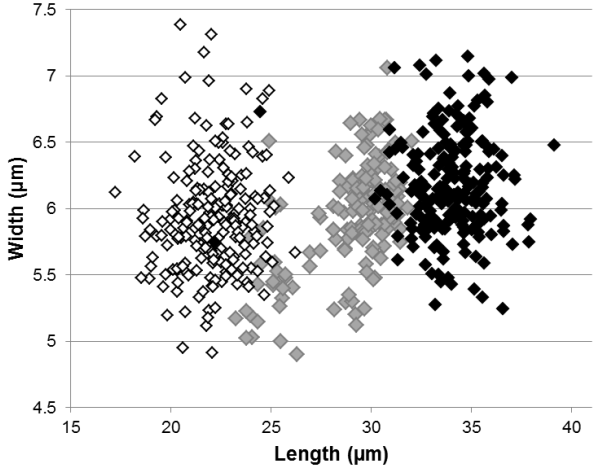
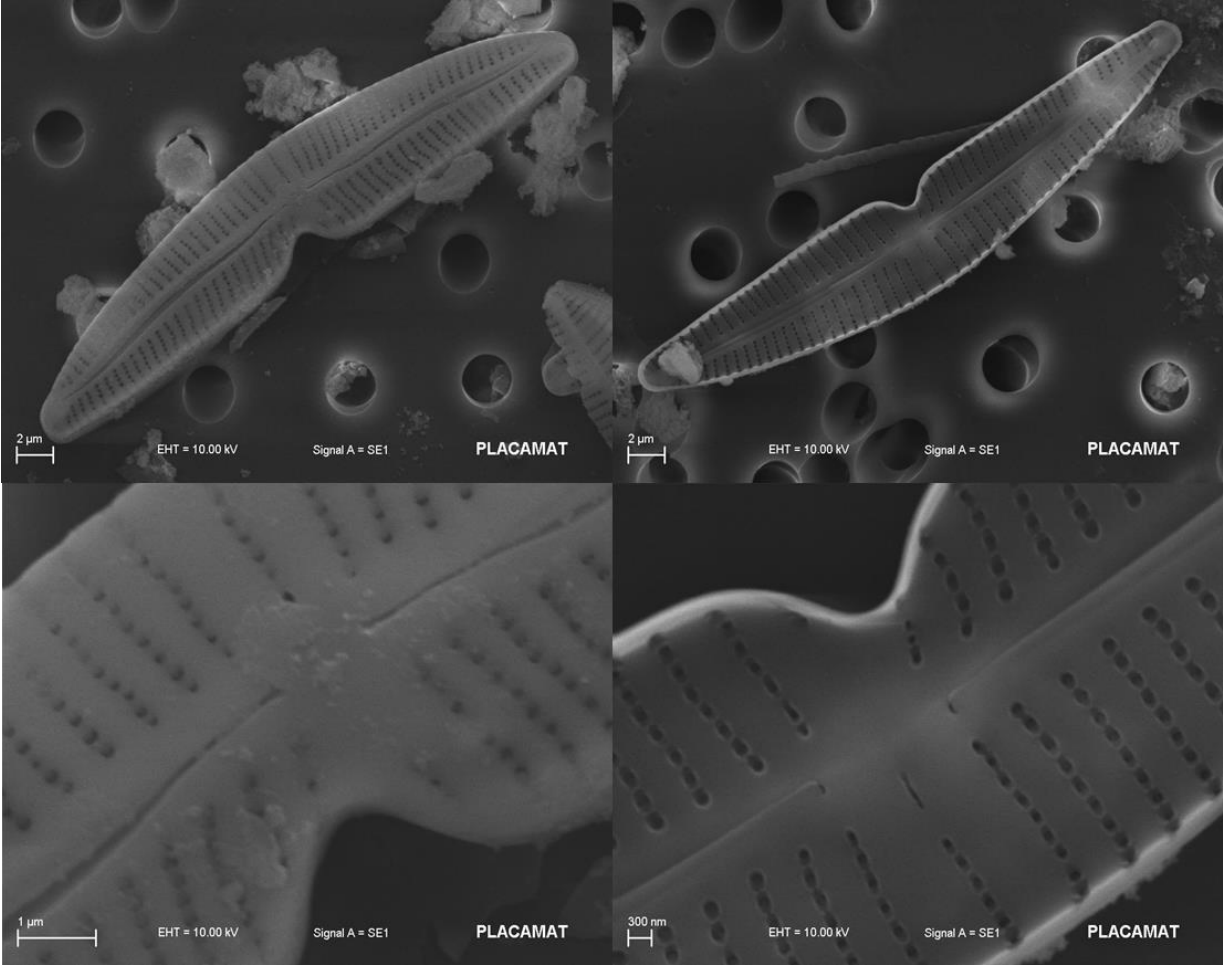
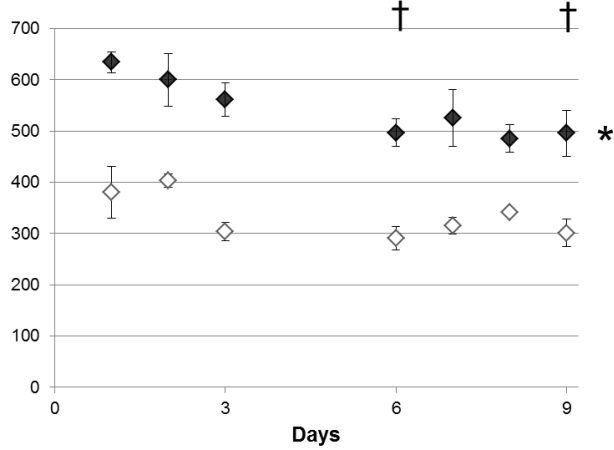


Fig. 2

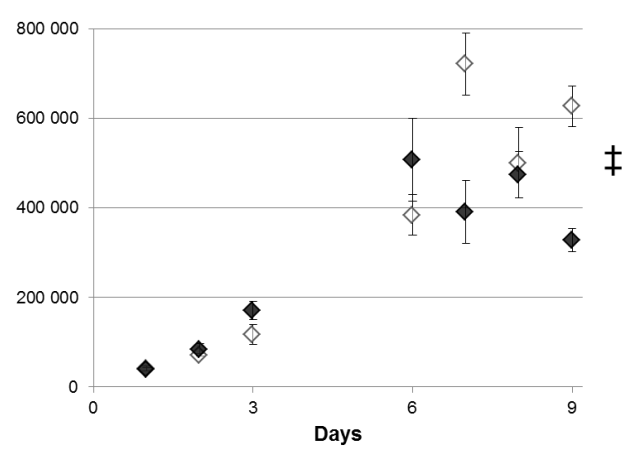


**Fig. 3**

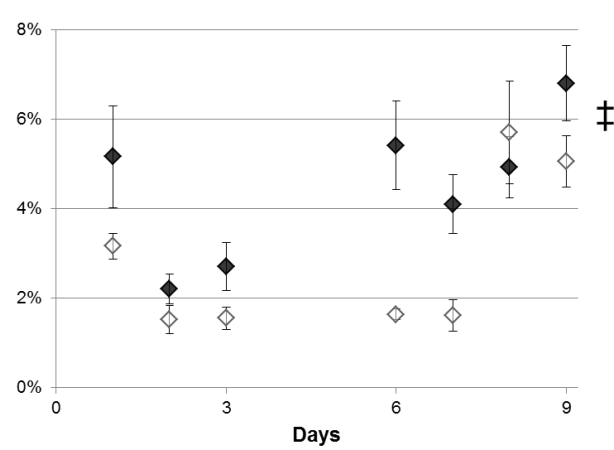
**A- Measured cell biovolume ( $\mu\text{m}^3$ )**



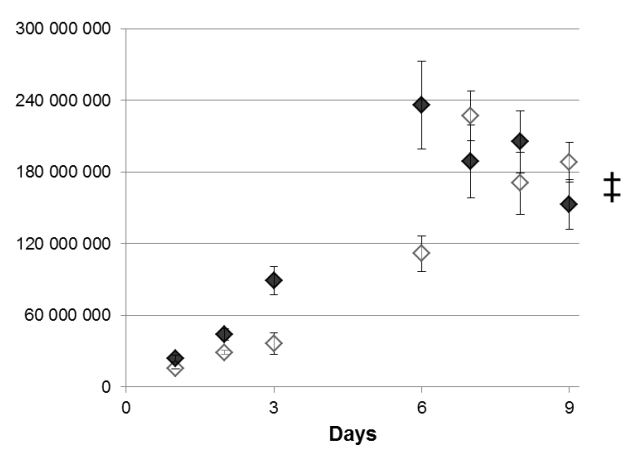
**B- Cell density ( $\text{cell.mL}^{-1}$ )**



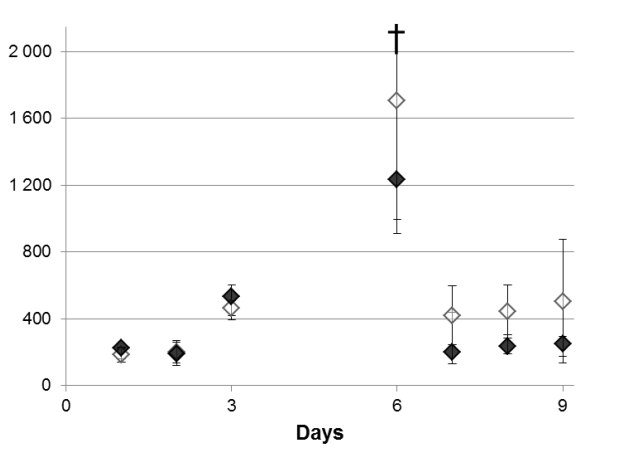
**C- Mortality**



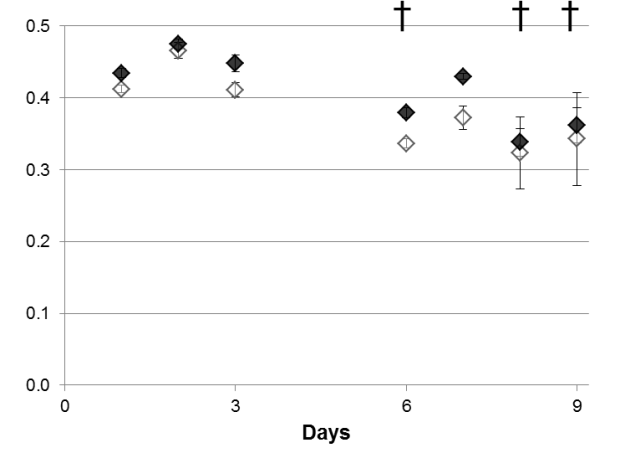
**D- Total biovolume ( $\mu\text{m}^3.\text{mL}^{-1}$ )**



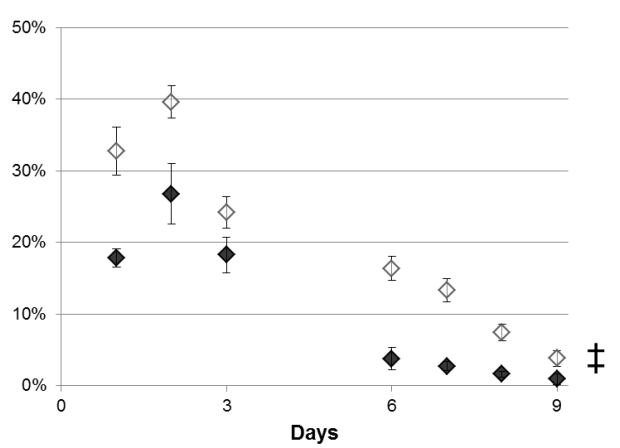
**E- Chlorophyll a concentration ( $\mu\text{g.cm}^2$ )**



**F- Photosynthetic efficiency (r.u.)**



**G- Cells in association**



**H- Mobile cells**

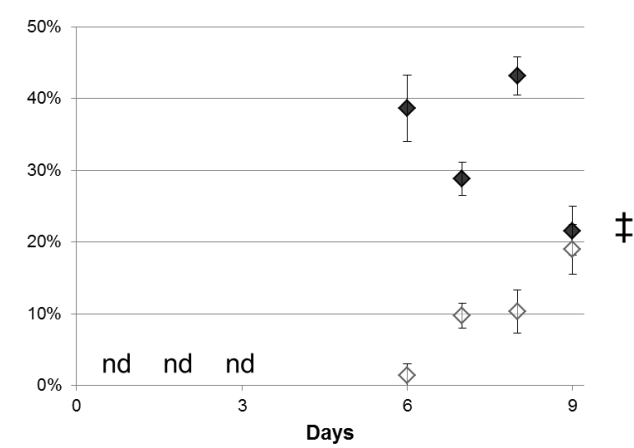


Fig. 4

Teratological forms

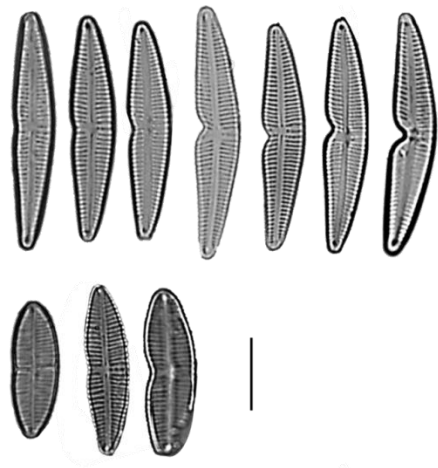
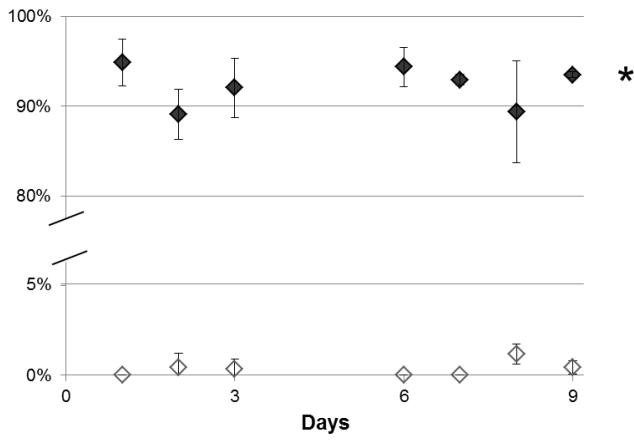
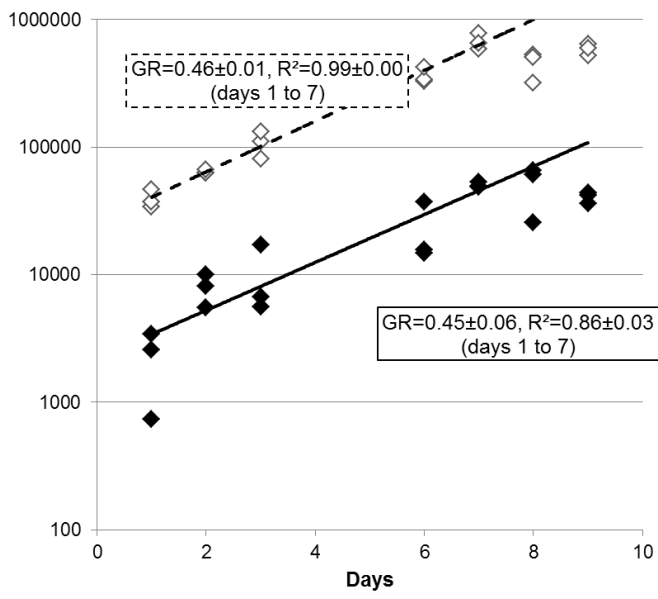
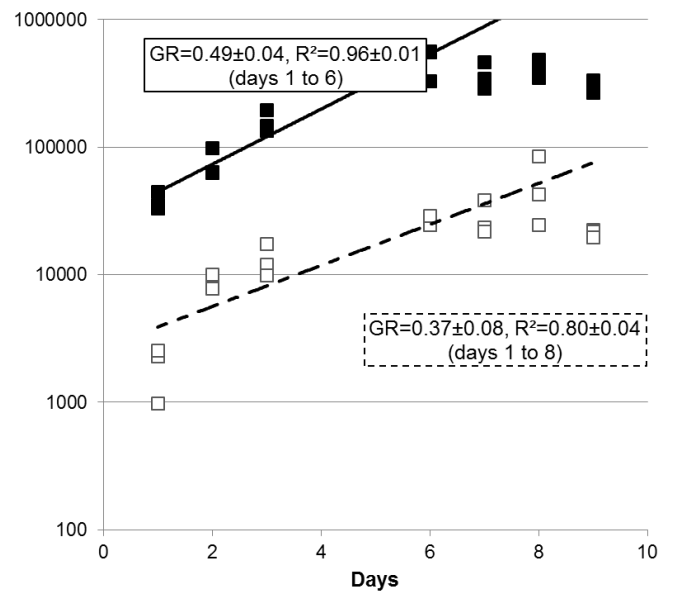


Fig. 5

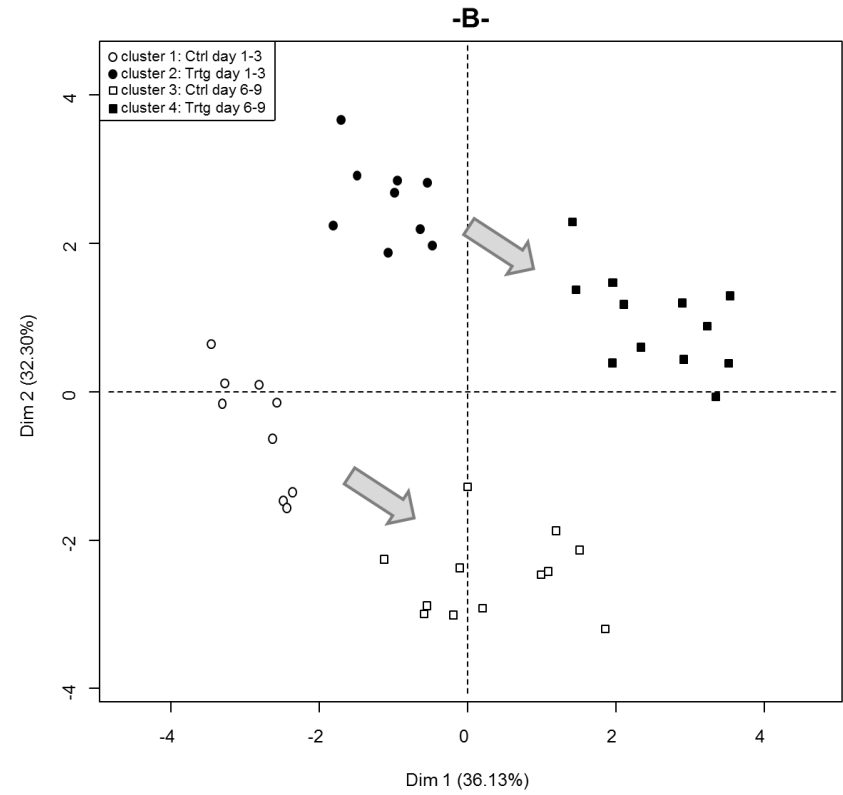
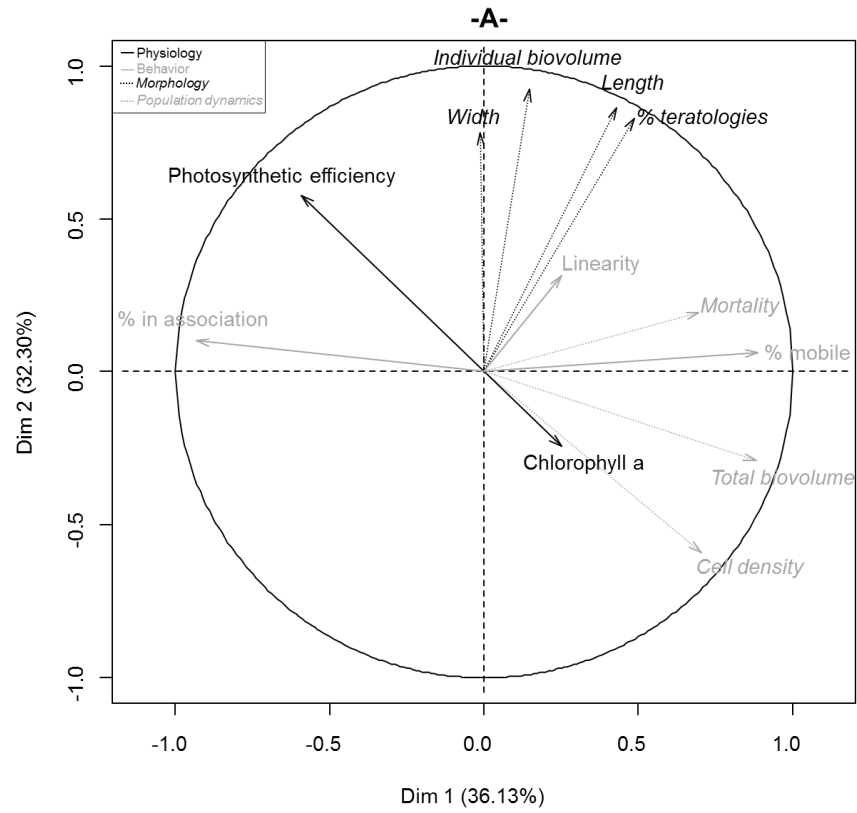
A- Cell densities (cell.mL<sup>-1</sup>) in Ctrl cultures



B- Cell densities (cell.mL<sup>-1</sup>) in Trtg cultures



1 Fig. 6

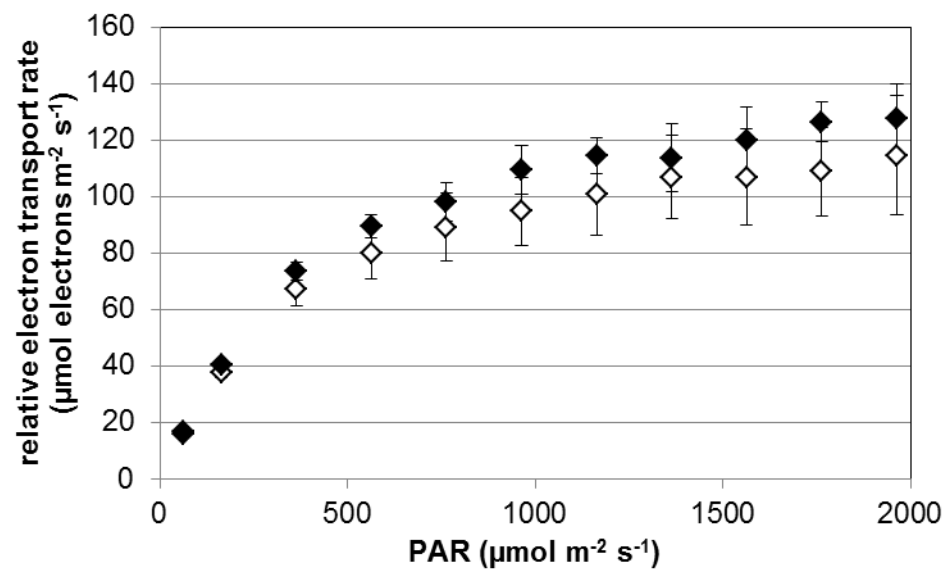


2  
3

**Appendix 1.** Characteristics of the diatom cultures analyzed in this study (Ctrl and Trtg) compared to the control cultures (GGRA) used in Coquillé et al. (2015). All values are mean  $\pm$  standard error over the experiment, except \* corresponding to the stationary phase and † that were only measurable on days 6 to 9; n=number of individuals measured/counted, N= number of samples. <sup>£</sup>: GGRA values are from Coquillé et al. (2015; control cultures). Effects of Culture, Date and Interaction between culture and date result from modelling; n.s.: not significant.

	Ctrl	Trtg	Culture effect	Date effect	Interaction	GGRA
<b>Morphology</b>						
Length ( $\mu\text{m}$ )	21.92 $\pm$ 0.09 (n=420)	33.88 $\pm$ 0.10 (n=420)	$p < 0.001$	n.s.	n.s.	28.91 $\pm$ 0.12 (n=300)
Width ( $\mu\text{m}$ )	5.92 $\pm$ 0.03 (n=210)	6.17 $\pm$ 0.03 (n=210)	n.s.	$p < 0.05$	n.s.	5.94 $\pm$ 0.04 (n=150)
Cell biovolume ( $\mu\text{m}^3$ )	334 $\pm$ 11 (n=210)	543 $\pm$ 16 (n=210)	$p < 0.001$	$p < 0.05$	n.s.	457 $\pm$ 14 (n=150)
Cells with abnormal outline (%)	0.34 $\pm$ 0.12 (n=2617)	92.32 $\pm$ 0.74 (n=2693)	$p < 0.001$	n.s.	n.s.	0.25 $\pm$ 0.12 (n=1571)
<b>Population dynamics</b>						
Cell density ( $10^3 \text{cells.mL}^{-1}$ )	616.2 $\pm$ 44.4* (N=9)	397.8 $\pm$ 31.7* (N=9)	n.s.	$p < 0.001$	$p < 0.001$	421.0 $\pm$ 42.7* (N=3)
Total biovolume ( $10^6 \mu\text{m}^3.\text{mL}^{-1}$ )	195.3 $\pm$ 20.3* (N=9)	198.6 $\pm$ 23.4* (N=9)	n.s.	$p < 0.001$	$p < 0.01$	210.1 $\pm$ 31.1* (N=3)
Mortality (%)	2.9 $\pm$ 0.4 (N=21)	4.5 $\pm$ 0.4 (N=21)	n.s.	$p < 0.05$	$p < 0.05$	1.1 $\pm$ 0.7 (N=24) <sup>£</sup>
<b>Physiology</b>						
Photosynthetic efficiency (r.u.)	0.38 $\pm$ 0.00 (N=21)	0.41 $\pm$ 0.00 (N=21)	n.s.	$p < 0.05$	n.s.	0.37 $\pm$ 0.00 <sup>£</sup> (N=24)
Chlorophyll-a concentration ( $\mu\text{g.cm}^{-2}$ )	561 $\pm$ 143 (N=21)	410 $\pm$ 87 (N=21)	n.s.	$p < 0.001$	n.s.	732 $\pm$ 155 <sup>£</sup> (N=24)
<b>Behaviour</b>						
Cells in association (%)	19.6 $\pm$ 5.4 (N=21)	10.3 $\pm$ 4.3 (N=21)	$p < 0.001$	$p < 0.01$	$p < 0.01$	9.76 $\pm$ 1.47 <sup>£</sup> (N=24)
Mobile cells (%)	10.1 $\pm$ 2.2 <sup>†</sup> (N=12)	33.0 $\pm$ 2.9 <sup>†</sup> (N=12)	$p < 0.001$	$p < 0.05$	$p < 0.01$	36.2 $\pm$ 4.6 <sup>£</sup> (N=24)
Linearity	0.85 $\pm$ 0.02 <sup>†</sup> (N=10)	0.90 $\pm$ 0.02 <sup>†</sup> (N=12)	$p < 0.05$	n.s.	n.s.	0.91 $\pm$ 0.01 <sup>£</sup> (N=24)
VAP ( $\mu\text{m.s}^{-1}$ )	2.7 $\pm$ 0.2 <sup>†</sup> (N=10)	3.5 $\pm$ 0.2 <sup>†</sup> (N=12)	n.s.	n.s.	n.s.	7.9 $\pm$ 0.2 <sup>£</sup> (N=24)
VSL ( $\mu\text{m.s}^{-1}$ )	2.3 $\pm$ 0.3 <sup>†</sup> (N=10)	3.1 $\pm$ 0.3 <sup>†</sup> (N=12)	n.s.	n.s.	n.s.	6.8 $\pm$ 0.2 <sup>£</sup> (N=24)
VCL ( $\mu\text{m.s}^{-1}$ )	2.9 $\pm$ 0.2 <sup>†</sup> (N=10)	3.7 $\pm$ 0.2 <sup>†</sup> (N=12)	n.s.	n.s.	n.s.	8.5 $\pm$ 0.2 <sup>£</sup> (N=24)

Appendix 2. Rapid Light Curves for Ctrl (white diamonds) and Trtg (black diamonds) cultures on day 9. Values are mean±standard errors of three replicates.





Appendix 3. PCR-ARISA patterns of amplified bacterial fragments in the replicate samples (Ctrl cultures: Ctrl\_1 to 3, Trtg cultures: Trtg\_1 to 3). Ref stands for the internal standards. Band intensity and position represent the ARISA peak intensity and corresponding migration duration [s] or fragment size [bp].

